# 2025.

**Reversible laser-assisted transformations of chalcogenide photonic media.** — Bulk $As_2S_3$ glass is dominated by network structures with only minor cage-like molecular inclusions, whereas freshly thermally evaporated arsenic-sulfur (As-S) thin films primarily consist of $As_4S_4$ and $As_4S_5$ molecular cages [1]. Thermal annealing or white-light irradiation polymerizes these cages, driving the films toward a bulk-like structure. In contrast, near-bandgap laser irradiation induces specific rearrangements of $As_4S_4$ cages, corresponding to the realgar-pararealgar transformation, which can be reversibly cycled through alternating laser exposure and thermal annealing.

The work further demonstrates controlled growth of As-S microcrystallites using thermally activated, gold nanoparticle-assisted synthesis (**Figure 1a**). By tuning synthesis conditions, selective formation of crystallites composed exclusively of photosensitive $As_4S_4$ or $As_4S_5$ molecules was achieved [2]. Raman spectroscopy, supported by DFT calculations, enabled precise identification of crystallite structures and *in-situ* monitoring of laser-induced transformations (**Figure 1b**). While $As_4S_5$ crystallites are stable under laser irradiation, $As_4S_4$ crystallites exhibit pronounced and reversible photoinduced structural changes.

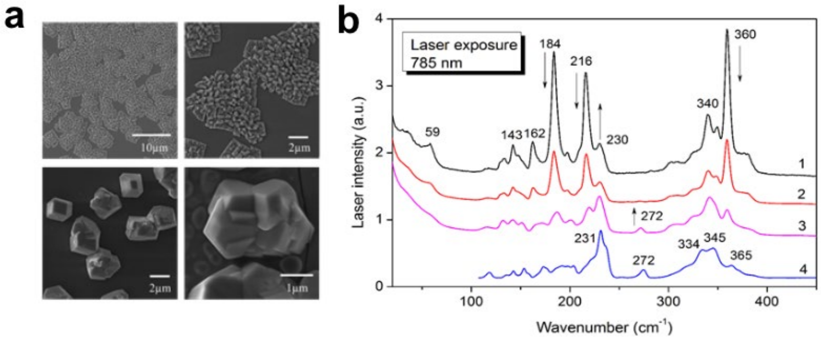

**Figure 1. (a)** Photosensitive $As_4S_4$ crystallites synthesized on Si wafers coated with gold NPs and maintained at 353 K, **(b)** *In-situ* structural transformations in the exposure-dependent Raman spectra of $As_4S_4$ crystallites excited by a 785 nm laser operating at constant intensity ($I_5=5.1\times10^5$ W/cm$^2$): 1) reference spectrum ($I_1=1.0\times10^4$ W/cm$^2$), 2) $t_1=2$ min, 3) $t_2=5.7$ hr. Raman spectrum of pararealgar [3] (4) is shown for comparison.

***References***
[1] https://doi.org/10.1007/978-94-024-2316-7_24.
[2] https://doi.org/10.1016/j.jallcom.2021.162467
[3] https://doi.org/10.1016/0584-8539(96)01698-4

**Wavelength-dependent femtosecond laser-induced structural changes in ultra-nanocrystalline diamond studied by Raman spectroscopy.** — Structural modifications of ultra-nanocrystalline diamond (UNCD) induced by femtosecond (fs) laser irradiation at two near-infrared wavelengths (800 nm (1.55 eV) and 950 nm (1.31 eV)) across a broad power range up to 160–164 mW were systematically investigated. The UNCD film of 1 μm thickness, consisting of nanocrystallites of a few hundred nm, was treated in a laser scanning microscope setup delivering ~2000 pulses per spot with a 1 μm focus. Post-irradiation analysis employed ultraviolet (325 nm) Raman spectroscopy and scanning electron microscopy (SEM). While SEM revealed no morphological changes even at maximum powers (energy densities ~0.5 $J/cm^2$), Raman spectra—decomposed via Gaussian fitting—showed pronounced wavelength- and power-dependent alterations in diamond (1332 $cm^{-1}$), graphitic G (1580 $cm^{-1}$), disorder-related D (1350 $cm^{-1}$), and grain-boundary bands.

Up to 140 mW, the diamond-to-graphitic G band intensity ratio exhibited subtle, opposing trends (**Figure 1**): a slight decrease at 800 nm (suggesting minor $sp^3$ loss) and increase at 950 nm, underscoring the material's sensitivity to small photon energy differences (0.24 eV). Above this threshold, the ratio rose sharply, which can be attributed primarily to recrystallization of intergrain $sp^2$ carbon into diamond-like $sp^3$ structures, as ablation was ruled out by SEM. The diamond peak position shifted oppositely with power: initial upshift (compressive stress) followed by downshift at 800 nm, versus monotonic upshift at 950 nm, corroborated by silicon substrate peak shifts (from 519.7 to 519.35 $cm^{-1}$ at 800 nm), linked to wavelength-dependent substrate absorption.

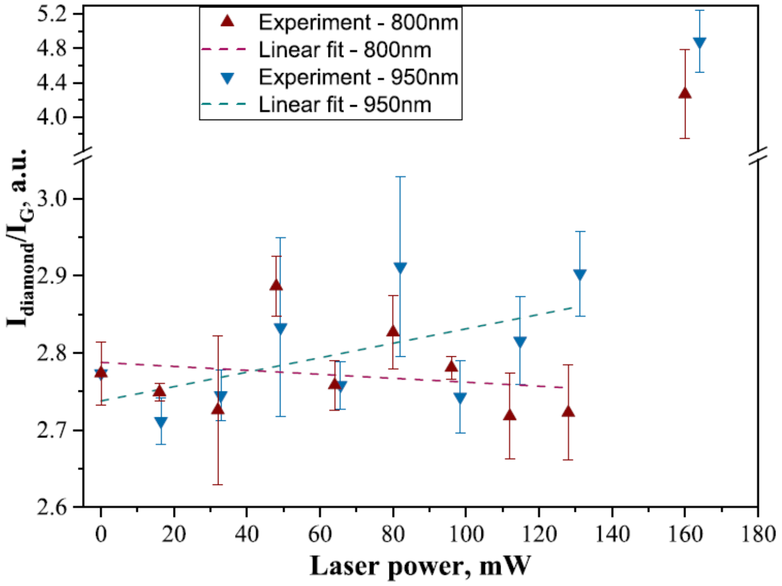

**Figure 1.** Change in the $I_{diamond}/I_G$ ratio in the Raman spectra of UNCD treated with 800 nm and 950 nm fs-lasers at different power levels.

The G-peak upshifts to 1581–1581.5 $cm^{-1}$ up to power thresholds of 112 mW (800 nm) and 102 mW (950 nm) indicating laser-driven graphitization via hydrogen desorption, $sp^3 \rightarrow sp^2$ conversion, and aromatic ring formation (**Figure 2**). Beyond these, G-peak downshifts and the $I_D/I_G$ ratio decreases, showing thermal breakdown of graphitic domains into disordered carbon. These findings delineate distinct regimes of stress evolution, graphitization, and structural breakdown, providing a foundation for precise fs-laser engineering of UNCD for photonics, THz devices, and color-center applications. [1]

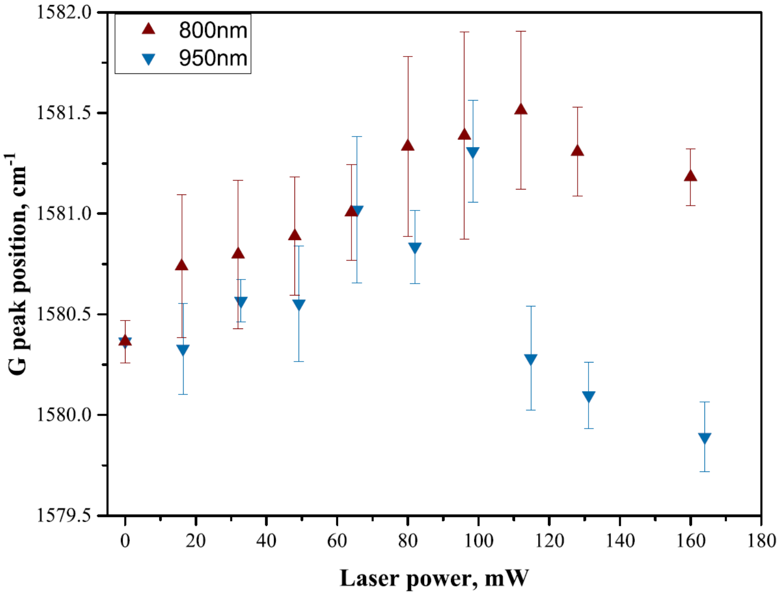

**Figure 2.** Change of the G peak position in the Raman spectra treated with 800 nm and 950 nm fs-lasers with different power levels.

***References***

[1] https://doi.org/10.1016/j.diamond.2025.112746

**Identification of DNA sequences and single-nucleotide polymorphisms by Raman spectroscopy.** — Accurate identification of nucleic acid sequences is essential for detecting RNA viruses and pathogenic DNA mutations. In particular, single-nucleotide variants (SNVs), including single-nucleotide polymorphisms (SNPs), are important biomarkers for numerous diseases, including cancer. Raman spectroscopy offers molecular-level structural information but its application to nucleic acid analysis is limited by low scattering cross-sections and spectral overlap of biomolecular vibrations. To overcome these limitations, a bioorthogonal Raman-labeling strategy based on alkyne-modified nucleotides is proposed. Alkynes exhibit strong Raman activity and characteristic C≡C stretching vibrations in the biologically silent spectral region (~1800 – 2800 $cm^{-1}$), enabling high specificity without spectral interference [1]. Their small size minimizes perturbation of native biomolecular interactions (**Figure 1, a,b**).

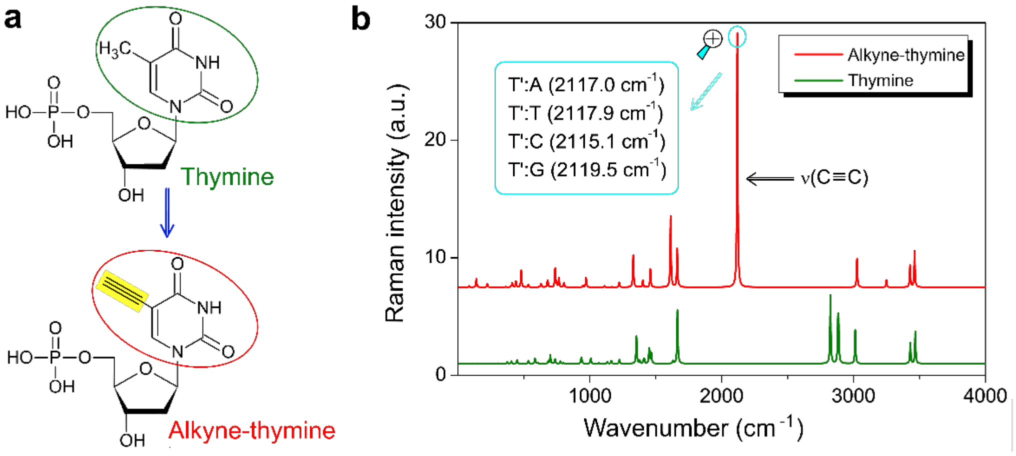

**Figure 1.** Modification of thymine **(a)** and simulated Raman spectra of thymine and alkyne-modified thymine molecules **(b)**. The inset shows the calculated C≡C stretching vibrational frequencies for different base pairs (T′ – alkyne-modified thymine).

Using *ab initio* calculations, it is shown that the alkyne vibrational frequency of a modified nucleotide is sensitive to hydrogen-bonding interactions with complementary bases [1]. This effect was experimentally confirmed in synthetic DNA containing 5-ethynyl-2′-deoxyuridine (EdU), where the C≡C stretching frequency of modified thymidine is unique for different base pairs (T′:A, T′:T, T′:C, and T′:G). This methodology enabled sequence-level identification of nucleic acids and detection of single-nucleotide mutations using high-precision Raman spectroscopy [2], including the BRAF V600E mutation associated with prostate cancer and the N-gene region of the SARS-CoV-2 genome. The results demonstrate the potential of alkyne-based Raman tagging for highly specific, label-assisted DNA diagnostics and sequence-resolved biomolecular detection.

## ***References***

[1] https://ssrn.com/abstract=6034463 or http://dx.doi.org/10.2139/ssrn.6034463.
[2] https://www.freepatentsonline.com/y2024/0011078.html